Radiative MHD Third Grade Nanofluid Flow Over a Stretching Cylinder with Prescribed Heat and Mass Fluxes

V.Nagendramma[1] A.Leelaratnam[2]

[1]Research Scholar, Department of Applied Mathematics, SPMVV, Tirupati, A.P., India

[2]Professor, Department of Applied Mathematics, SPMVV, Tirupati, A.P., India

Abstract— *Present article reports steady two dimensional effects of heat and mass transfer flow of MHD third grade fluid over a stretching cylinder with nanoparticles embedded in a porous medium. Formulation of the problem and relevant numerical analysis are given with thermal radiation and uniform heat source/sink with prescribed heat and mass flux conditions. The non linear partial differential equations are transformed into a system of ordinary differential equations by using Runge-Kutta-Fehlberg method. The impact of emerging parameters viz, the Hartmann number* M, *the permeability parameter* k, *the curvature parameter* γ, *the material parameters* α_1^* and α_2^*, *the fluid parameter* β, *the Reynolds number* Re, *the Prandtl number* Pr, *the Brownian motion parameter* Nb, *the thermophoresis parameter* Nt, *the thermal radiation parameter* Nr, *the heat source/sink parameter* δ *and the Lewis number* Le *on velocity, temperature ad nanoparticle volume fraction are examined. Interesting results are delineated through graphs.*

Keywords — *MHD, heat source/sin, third grade nanofluid, thermal radiation, stretching cylinder.*

NOMENCLATURE

u, v : Velocity components in x and y directions

x : Direction along the surface

r : Direction normal to the surface

R : Radius of the cylinder

u_w : Linear stretching velocity

l : Reference length

u_0 : Reference velocity

α_1, α_2 and β_3 : Material parameters

K : Permeability parameter of the porous medium

B_0 : Dimensional magnetic field parameter

k_T : Thermal conductivity

T : Temperature of the fluid

T_w : Wall temperature

T_∞ : Temperature of the fluid in free stream

D_B : Brownian diffusion coefficient

D_T : Thermophoresis diffusion coefficient

Q_0 : Heat generation/absorption coefficient

C : Concentration of the fluid

C_f : Skin friction coefficient

C_p : Specific heat capacity at constant pressure

C_w : Reference concentration

C_∞ : Concentration of the fluid in free stream

f : Dimensionless velocity

M : Hartmann number $\left(\frac{\sigma B_0^2 l}{\rho u_0}\right)$

k : Permeability parameter $\left(\frac{\nu l}{K u_0}\right)$

α_1^* : fluid parameter $\left(\alpha_1^* = \frac{\alpha_1 u_0}{\mu l}\right)$

α_2^* : fluid parameter $\left(\alpha_2^* = \frac{\alpha_2 u_0}{\mu l}\right)$

β : fluid parameter $\left(\beta = \frac{\beta_3 {u_0}^2}{\mu l^2}\right)$

Nb : Brownian motion parameter $\left(Nb = \frac{\tau D_B C_\infty}{\nu}\right)$

Nt : Thermophoresis parameter $\left(Nt = \frac{\tau D_T \Delta T}{T_\infty \nu}\right)$

Pr : Prandtl number $\left(\Pr = \frac{\nu}{\sigma}\right)$

Le : Lewis number $\left(Le = \frac{\nu}{D_B}\right)$

Nr : Thermal radiation parameter $\left(Nr = \frac{16\sigma^* T_\infty^3}{k_T k^*}\right)$

Re_x : Local Reynolds number

C_f : Shear stress coefficient

Nu_x : Local Nusselt number

Sh_x : Local Sherwood number

Greek Symbols

η : Similarity variable

ϕ : Dimensionless concentration

σ : Electrical conductivity of the fluid

τ : Ratio of specific heats

γ : Curvature parameter $\left(\gamma = \sqrt{\frac{l\nu}{a^2 U_0}}\right)$

θ : Dimensionless temperature

ρ : Density of the fluid

μ : Dynamic viscosity

υ : Kinematic viscosity

δ : Heat source/sink parameter $\left(\delta = \frac{Q_0 l}{\rho c_p u_0}\right)$

I. INTRODUCTION

In our day to day life, some fluids reveal the mechanical attributes of both viscosity and elasticity. These fluids are called as non-Newtonian fluids. These fluids cannot be expounded by the theoretical concepts of viscosity or elasticity but can be explained by an amalgamation of both. Due to rheological nature of non-Newtonian fluids several constitutive equations are propounded [1]. In most of the fluid food materials, the stress is dependent on the shear rate. Non-Newtonian fluids include in performance of lubricants, wire and fiber coating, food processing, movement of biological fluids, transpiration cooling, gaseous diffusion, drilling mud, heat pipes etc. Third grade fluid is a subclass of non-Newtonian fluids and its equation is based on non linear relation between stress and strain is. Hayat et al. [2] studied a steady, incompressible third grade fluid flow through a rotating frame in the presence of magnetohydrodynamics. The incompressible third-grade fluid due to a helical screw rheometer is investigated by Zed et al. [3] by unwrapping the channel, lands and the outsider rotating barrel. They considered that the shallow infinite channel as a geometry of the flow and its width is more than depth of the shallow. Majhi and Nair [4] explored results on stenotic geometry of non-Newtonian third grade fluid over stenosed tubes on the resistive impedance and wall shear stress. Taza Gul et al. [5] perused a steady, two dimensional laminar thin film flow of MHD third grade fluid over a vertical belt subject to temperature dependent viscosity. Rehman et al. [6] investigated mixed convection stagnated boundary layer flow and heat transfer characteristics of third grade fluid past an exponentially stretching sheet.

The phenomena of transport in porous media are encountered in many engineering disciplines. For example Civil engineering deals, with the flow of water in aquifers, the movement of moisture through and under engineering structures, transport of pollutants in aquifers and the propagation of stresses under foundations of structures. Nagendramma et al. [7] analysed triple diffusive MHD laminar boundary layer flow over a nonlinear stretching sheet embedded in a porous medium in the presence of velocity slip with nanoparticles. Manoj Kumar Nayak et al. [8] perused results on steady MHD viscoelastic fluid flow, heat and mass transfer characteristics past a stretching sheet embedded in a porous medium subject to chemical reaction. An analysis on unsteady magnetohydrodynamic boundary layer flow of nanofluid due to a channel with moving porous walls and medium is probed by Muhammad Zubair Akbar et al [9]. Ali Montakhab [10] explored results on convective heating or cooling characteristics of porous media which has applications in the design of thermal energy storage systems. Alibakhsh Karsein et al [11] reviewed results on non-Newtonian nanofluid flow subject to magnetohydrodynamic effect through porous media.

It is deeply-ingrained that the convective heat and mass transfer confined in the form of thermal and solutal boundary conditions is defined with prescribed temperature and concentration fluxes on the surface of the boundary, this occurs in many situations, especially in cooling of electrical and nuclear components, with the prescribed heat flux. Prescribed heat flux plays pivotal role when overheating, burnout and meltdown are major issues. Abbasi et al. [12] reviewed impact of heat and mass flux boundary conditions of Jeffrey fluid hydro magnetic flow over a stretching sheet in the presence of thermal radiation with nanoparticles. Hayat et al. [13] investigated impact of viscous dissipation and ohmic effects on a three dimensional laminar flow of nanofluid with prescribed temperature and concentration fluxes. Majeed et al. [14] explored results on steady, heat transfer characteristics of non-Newtonian Casson fluid flow through a stretching cylinder with prescribed heat flux in the presence of partial slip.

The present study addresses the steady MHD radiative two dimensional boundary layer flow of third grade nanofluid due to a stretching cylinder with heat source/sink. Heat and mas transfer effects are analyzed through prescribed nanoparticle temperature and prescribed nanoparticle mass flux boundary conditions are considered. Formulation of the problem is made with appropriate boundary layer approximations. To develop energy equation Rosseland approximation is employed for thermal radiation. Results are investigated through Runge-Kutta-Fehlberg method with shooting technique. Solution expressions are studied through graphs and tabular values for disparate controlling quantities.

II. THIRD GRADE NON-NEWTONIAN FLUID RHEOLOGICAL MODEL:

Present investigation describes a sub class of non-Newtonian fluids called Third grade fluid. The constitutive equation of Third grade fluid can be defined as follows

$$T = -pI + \mu A_1 + \alpha_1 A_2 + \alpha_2 A_1^2 + \beta_3 \left(trA_1^2\right) A_1 \qquad (1)$$

Where T is the Cauchy stress tensor, p is the hydrostatic pressure, μ is the dynamic viscosity, I is the identity tensor and $\alpha_i \ (i = 1,2)$ and $\beta_j \ (j = 1,2,3)$ are material constants. Furthermore, thermodynamics imposes the following constraints [15]: $\mu \geq 0,\ \alpha_1 \geq 0,\ |\alpha_1 + \alpha_2| \leq \sqrt{24\mu\beta_3},\ \beta_1 = \beta_2 = 0, \beta_3 \geq 0$ (2)

III. MATHEMATICAL FORMULATION

Consider the 2D laminar flow of magnetohydrodynamic third grade fluid. The fluid flow is driven through a stretching cylinder. The $x-$ axis is measured along the flow direction and radial axis normal to the cylinder. We assumed that the strength of the magnetic field is applied normal to the direction of the flow and an induced magnetic field is negligible, when the magnetic Reynolds number is lckle. The surface is maintained uniform and prescribed temperature and concentration fluxes q_w and m_w are considered respectively. In addition, the nanoparticle volume fraction on the ambient is envisaged to obey the passively controlled model suggested by Kzunestov and Nield [16]. Under these presumptions the appropriate transport equations are stated as follows

$$\frac{\partial}{\partial x}(ru)+\frac{\partial}{\partial r}(rv)=0 \qquad (3)$$

$$\rho\left(u\frac{\partial u}{\partial x}+v\frac{\partial u}{\partial r}\right)=\mu\left(v\frac{\partial^2 u}{\partial r^2}+\frac{1}{r}\frac{\partial u}{\partial r}\right)+$$

$$\alpha_1\begin{pmatrix}\frac{u}{r}\frac{\partial^2 u}{\partial r\partial x}+\frac{v}{r}\frac{\partial^2 u}{\partial r^2}+\frac{3}{r}\frac{\partial u}{\partial r}\frac{\partial u}{\partial x}\\ +\frac{1}{r}\frac{\partial u}{\partial r}\frac{\partial v}{\partial r}+4\frac{\partial u}{\partial r}\frac{\partial^2 u}{\partial r\partial x}+\\ u\frac{\partial^3 u}{\partial r^2\partial x}+2\frac{\partial v}{\partial r}\frac{\partial^2 u}{\partial r^2}+\\ v\frac{\partial^3 u}{\partial r^3}+3\frac{\partial^2 u}{\partial r^2}\frac{\partial u}{\partial x}+\frac{\partial^2 v}{\partial r^2}\frac{\partial u}{\partial r}\end{pmatrix}+$$

$$\alpha_2\begin{pmatrix}\frac{2}{r}\frac{\partial u}{\partial r}\frac{\partial v}{\partial r}+\frac{2}{r}\frac{\partial u}{\partial r}\frac{\partial u}{\partial x}+2\frac{\partial^2 v}{\partial r^2}\frac{\partial u}{\partial r}+\\ 2\frac{\partial^2 u}{\partial r^2}\frac{\partial v}{\partial r}+2\frac{\partial^2 u}{\partial r^2}\frac{\partial u}{\partial x}+4\frac{\partial^2 u}{\partial r\partial x}\frac{\partial u}{\partial r}\end{pmatrix} \qquad u\frac{\partial T}{\partial x}+v\frac{\partial T}{\partial r}=\frac{k_T}{\rho c_p}\left(\frac{\partial^2 T}{\partial r^2}+\frac{1}{r}\frac{\partial T}{\partial r}\right)+$$

$$+\beta_3\left(\frac{2}{r}\left(\frac{\partial u}{\partial r}\right)^3+6\left(\frac{\partial u}{\partial r}\right)^2\frac{\partial^2 u}{\partial r^2}\right)-\sigma B_0^2 u-\frac{\mu}{K}u \quad (4)\ \tau\left(D_B\left(\frac{\partial T}{\partial r}\frac{\partial C}{\partial r}\right)+\frac{D_T}{T_\infty}\left(\frac{\partial T}{\partial r}\right)^2\right)+ \qquad (5)$$

$$\frac{Q_0}{\rho c_p}(T-T_\infty)-\frac{1}{\rho c_p}\frac{\partial q_r}{\partial y}$$

$$u\frac{\partial C}{\partial x}+v\frac{\partial C}{\partial r}=D\left(\frac{\partial^2 C}{\partial r^2}+\frac{1}{r}\frac{\partial C}{\partial r}\right)+\frac{D_T}{T_\infty}\frac{1}{r}\frac{\partial}{\partial r}\left(r\frac{\partial T}{\partial r}\right) \qquad (6)$$

The boundary conditions are

$$u=u_w=\frac{u_0 x}{l},\ v=0,\qquad \text{at } r=R \quad (7)$$
$$k_T\frac{\partial T}{\partial r}=-q_w(x),\ D_B\frac{\partial C}{\partial r}=-m_w(x)$$

$$u\to 0,\ T\to T_\infty, C\to C_\infty \text{ at } r\to\infty \qquad (8)$$

IV. SIMILARITY TRANSFORMATION OF MATHEMATICAL MODEL

To proceed, the following similarity variables are introduced

$$\eta=\sqrt{\frac{u_0}{\nu l}}\left(\frac{r^2-R^2}{2R}\right), u=u_w f', v=-\frac{R}{r}\sqrt{\frac{u_0\nu}{l}}f,$$
$$T=T_\infty+\frac{q_w}{k_T}\sqrt{\frac{\nu x}{u_w}}\theta(\eta), C=C_\infty+\frac{m_w}{D_B}\sqrt{\frac{\nu x}{u_w}}\phi(\eta) \quad (9)$$

Eqn. (3) is automatically satisfied and since there is no longitudinal pressure gradient, employing Eqn. (9) we have transfigured Eqns. (4) – (6) into a set of ordinary differential equations

$$\begin{aligned}&(1+2\gamma\eta)f'''+2\gamma f''+ff''-(f')^2+\\&\alpha_1^*\begin{pmatrix}6\gamma f'f''+3(1+2\gamma\eta)(f'')^2-2\gamma ff'''\\+2(1+2\gamma\eta)f'f'''-(1+2\gamma\eta)ff''''\end{pmatrix}+\\&\alpha_2^*\begin{pmatrix}2\gamma ff'''+2\gamma f'f''\\+2(1+2\gamma\eta)(f'')^2\end{pmatrix}+\\&\beta\begin{pmatrix}8\gamma\,\mathrm{Re}(1+2\gamma\eta)^2(f'')^3+\\6\,\mathrm{Re}(1+2\gamma\eta)^2(f'')^2f'''\end{pmatrix}-(M+k)f'=0\end{aligned} \quad (10)$$

$$\begin{aligned}&((1+2\gamma\eta)+Nr)\theta''+2\gamma\theta'+\\&\mathrm{Pr}\begin{pmatrix}f\theta'-f'\theta+(1+2\gamma\eta)\theta'\phi'Nb+\\(1+2\gamma\eta)Nt\theta'^2+\delta\theta\end{pmatrix}=0\end{aligned} \quad (11)$$

$$\begin{aligned}&(1+2\gamma\eta)\phi''+2\gamma\phi'+Le(f\phi'-f'\phi)+\\&\frac{Nt}{Nb}(2\gamma\theta'+(1+2\gamma\eta)\theta'')=0\end{aligned} \quad (12)$$

The boundary conditions (7) and (8) are transmuted as

$$f'=1,\ f=0,\theta'=-1,\phi'=-1 \quad \text{at } r=R \quad (13)$$
$$f'\to 0,\theta\to 0,\phi\to 0 \quad \text{as } r\to\infty \quad (14)$$

The expressions for local shear stress, rate of heat transfer and mass transfer are given by

$$C_f=\frac{\tau_w}{\rho(u)^2}=\frac{(\tau_{rx})_{r=R}}{\rho(u)^2}, Nu_x=\frac{xq_w}{\alpha\Delta T}, Sh_x=\frac{xm_w}{D_B\Delta C} \quad (15)$$

$$\begin{aligned}&\tau_{rx}=\mu\frac{\partial u}{\partial r}+\alpha_1\left(u\frac{\partial^2 u}{\partial r\partial x}+v\frac{\partial^2 u}{\partial r^2}+3\frac{\partial u}{\partial r}\frac{\partial u}{\partial x}+\frac{\partial u}{\partial r}\frac{\partial v}{\partial r}\right)+\\&\text{where}\,\alpha_2\left(2\frac{\partial u}{\partial r}\frac{\partial v}{\partial r}+2\frac{\partial u}{\partial r}\frac{\partial u}{\partial x}\right)+2\beta_3\left(\frac{\partial u}{\partial r}\right)^3\end{aligned} \quad (16)$$

$$q_w=-k_T\left(\frac{\partial T}{\partial r}\right)_{r=R},\quad m_w=-D_B\left(\frac{\partial C}{\partial r}\right)_{r=R}$$

In non dimensional form, the Eqn. (15) can be expressed as

$$\begin{aligned}&C_f\,\mathrm{Re}_x^{1/2}=f''(0)++3\alpha_1^*f''(0)+2\beta f''^3(0),\\&\frac{Nu_x}{\mathrm{Re}_x^{1/2}}=\frac{1}{\theta(0)},\frac{Sh_x}{\mathrm{Re}_x^{1/2}}=\frac{1}{\phi(0)}\end{aligned} \quad (17)$$

where $\mathrm{Re}_x = \sqrt{\frac{a}{\upsilon l}}x$

V. Results and Discussion

Present discussion concentrates on the controlling parameters on velocity, temperature nanoparticle volume fraction. The behavior of the derived expressions for sundry parameters are elucidated graphically by utilizing a numerical technique i.e., Runge-Kutta-Fehlberg method along with appropriate software package Matlab R2015b.

Impact of third grade fluid parameters $\alpha_1^* \text{ and } \alpha_2^*$ on velocity distribution is illustrated in Figs. 1 and 2. There is a hike in velocity when $\alpha_1^* \text{ and } \alpha_2^*$ are enhanced. This is by the virtue of the fact that material parameters are inversely proportional to the viscosity. As $\alpha_1^* \text{ and } \alpha_2^*$ increase the fluid velocity diminishes and hence velocity magnifies. The temperature and nanoparticle volume fraction distributions are elucidated for various values of $\alpha_1^* \text{ and } \alpha_2^*$ in Figs. 3- 6. From this figures we notice that temperature and nanoparticle volume fraction are decreasing fields with increasing values of $\alpha_1^* \text{ and } \alpha_2^*$.

The variation of fluid parameter and Reynolds number on velocity are delineated in Figs. 7 and 8. This is seen that velocity enhances with the hike of fluid parameter and Reynolds number. Literally, Reynolds number is the ratio of inertial force to viscous force and hence inertial forces are more influential than the viscous forces when Re increased as a result velocity rises. The temperature and nanoparticle volume fraction are decelerate with higher values of $\beta \text{ and } \mathrm{Re}$ (Figs. 9-12).

Figs. 13-15 reveal the influence of Hartmann number (M) on velocity, temperature and nanoparticle volume fraction. It is clear that the raise in the strength of the magnetic field is to decrease the velocity, because the action of Lorentz force which thwarts the fluid motion. The impact of magnetic field on temperature is depicted in Fig. 14. It is found that temperature hikes with raising values of Hartmann number, since energy is dispelled as heat when the fluid flow is decelerated and thus provides enhancement in thermal boundary layer thickness. Impact of Hartmann number on nanoparticle volume fraction is qualitatively similar to that of temperature profile.

Fig. 16 elucidates that the velocity diminishes as the permeability parameter (k) enhances. This is in conformity with the fact the Darcy resistance offered by the porous medium. Larger values of permeability parameter correspond to considerable resistance to the fluid flow and therefore velocity diminishes. Fig.17 depicts the increasing values of k elevates the temperature and thermal boundary layer thickness. The nanoparticle volume fraction also allows the same phenomena with k (Fig. 18).

A cross over is seen in the velocity and temperature distribution at $\eta \approx 0.4$ as portrayed in Figs. 19 and 20. For the dynamic boundary, $\eta < 0.4$ the rise of γ tends to a reduction in the momentum boundary layer faintly, by the virtue of petit increment of the frictional forces by enhancing the surface shear stress whereas it shows inimical behavior at far away from the surface, $\eta > 0.4$. This is in conformity with the fact as γ enhances the cylinder shrinks and hence the space provided for fluid is increased at free stream. The nanoparticle volume fraction diminishes as γ enhances, due to the elevation of the surface mass flux (Fig. 21).

Fig. 22 is elucidated to notice the impact of Prandtl number (Pr) on temperature field. It is clearly portrays that temperature diminishes when Pr is enhanced. In fact, higher Prandtl number fluid has low thermal diffusivity which is responsible for the decrement of temperature. Fig.23 is the sketch of temperature field for a variation in thermal radiation parameter (Nr). Temperature and thermal boundary layer thickness enhance for higher values of Nr. Greater values of Nr yield more heat to the fluid which results in rise of temperature. Fig.24 delineates that temperature is enhanced in the presence of heat source. This is because heat source releases energy in the thermal boundary layer.

Fig. 25 is the plot for temperature distribution for the impact of Brownian motion parameter. Physically, Brownian motion generates micro-mixing, which hikes the thermal conductivity of the fluid as a result the temperature increases. The same behavior is seen on concentration with increasing Brownian motion parameter (Fig. 26). Fig. 27 and 28 elucidate the impact of thermophoretic parameter Nt on the temperature and nanoparticle volume fraction fields. In fact in the presence of thermophoresis the particles are driven towards cold surface from hot surface, hence the temperature and nanoparticle volume fraction enhance with a

rise in thermophoretic parameter Nt. The impact of Lewis number on nanoparticle volume fraction is displayed in Fig. 29. Physically, larger Lewis number implies that the molecular diffusivity of the fluid is small and therefore the concentration decreases.

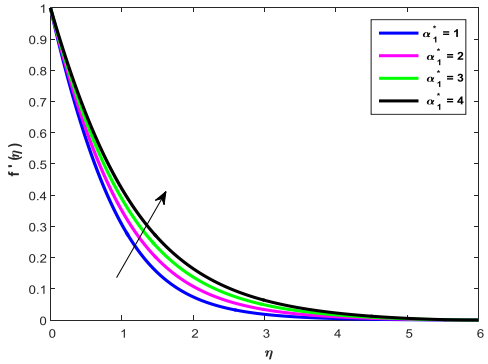

Fig.1: Velocity profile for different values of α_1^*

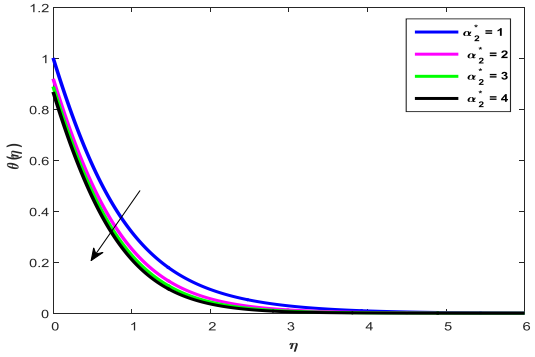

Fig. 4: Temperature profile for various values of α_1^*

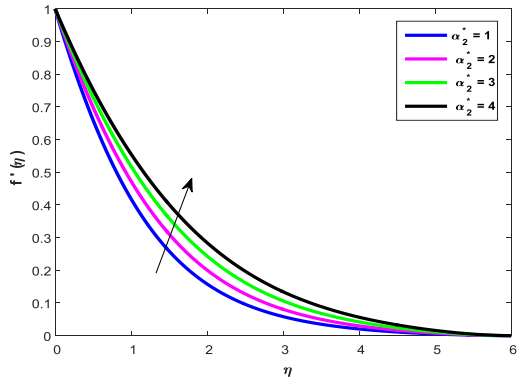

Fig. 2: Velocity profile for different values of α_2^*

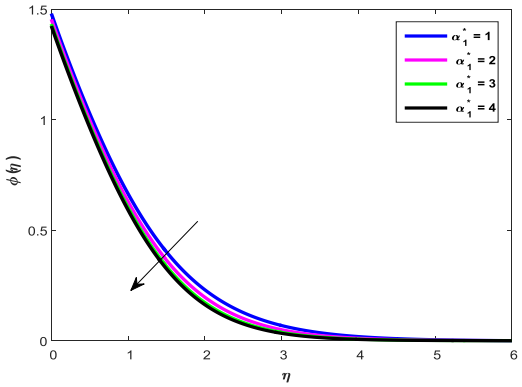

Fig. 5: Nano particle volume fraction profile for various values of α_1^*

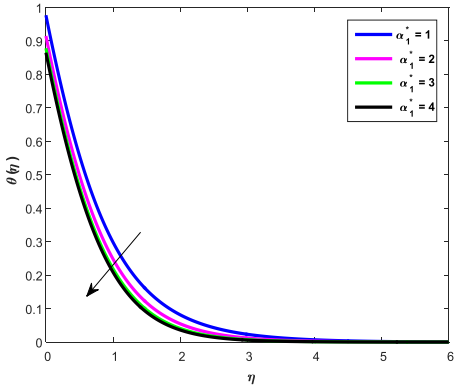

Fig. 3: Temperature profile for various values of α_1^*

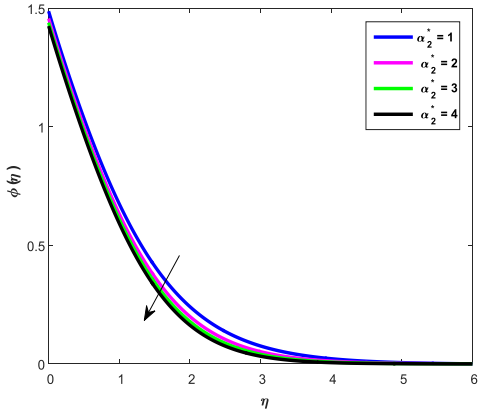

Fig. 6: Nano particle volume fraction profile for different values of α_2^*

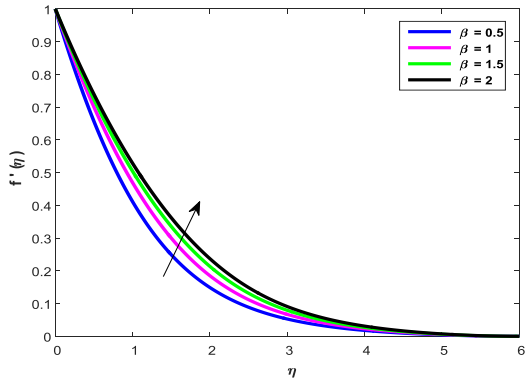

Fig. 7: Velocity profile for different values of β

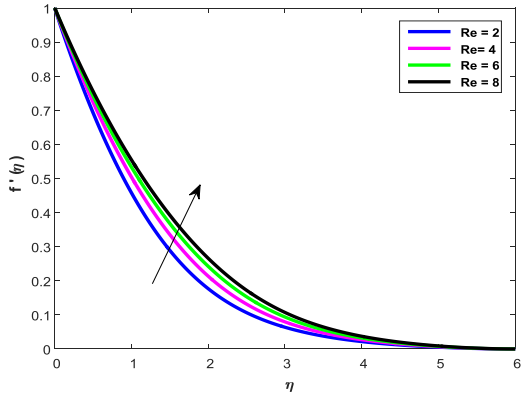

Fig. 8: Velocity profile for different values of Re

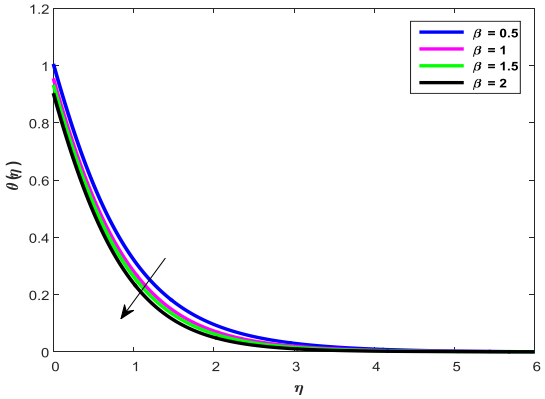

Fig. 9:Temperature profile for various values of β

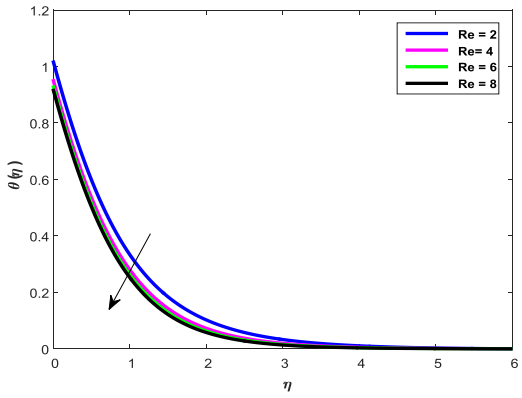

Fig.10:Temperature profile for various values of Re

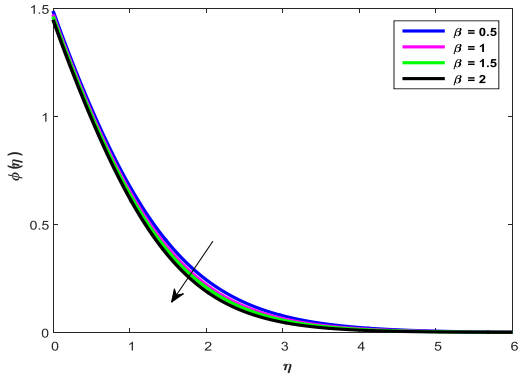

Fig. 11: Nano particle volume fraction profile for different values of β

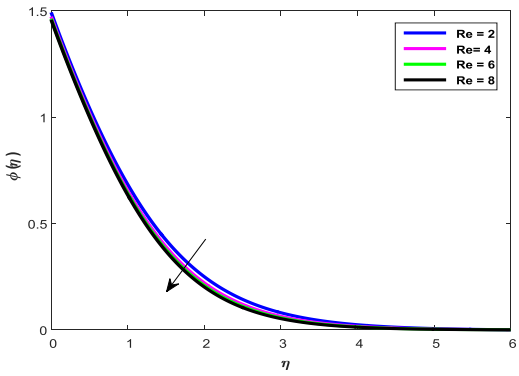

Fig. 12: Nano particle volume fraction profile for different values of Re

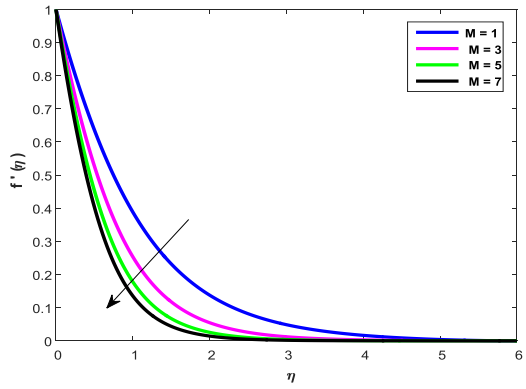

Fig. 13: Velocity profile for different values of M

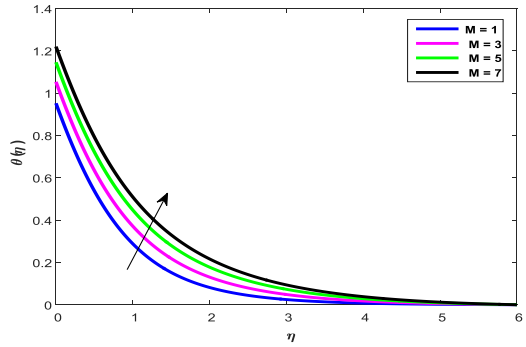

Fig.14:Temperature profile for various values of M

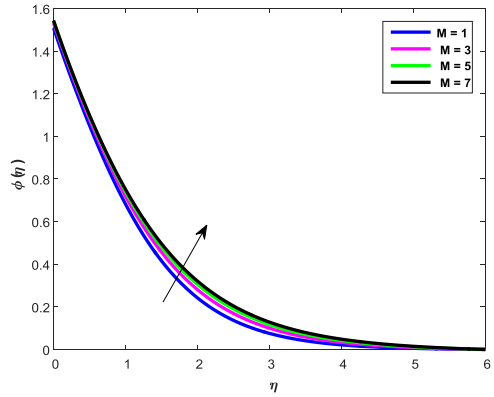

Fig. 15: Nanoparticle volume fraction profile for different values of M

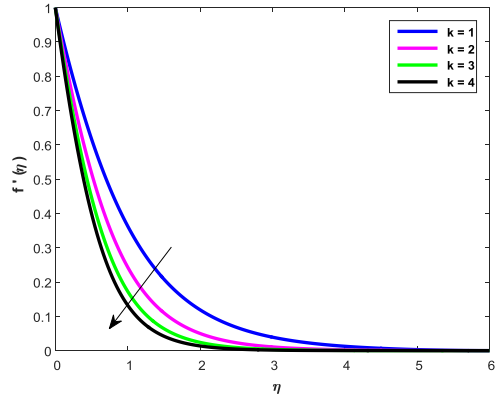

Fig. 16: Velocity profile for different values of k

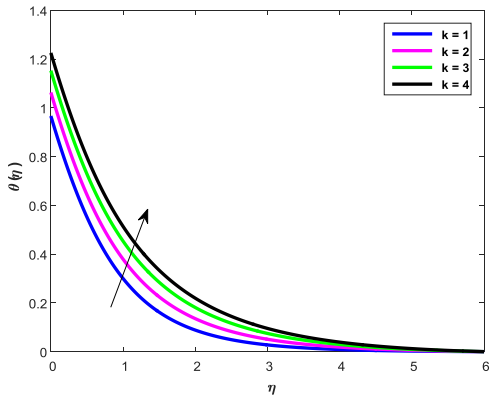

Fig.17:Temperature profile for various values of k

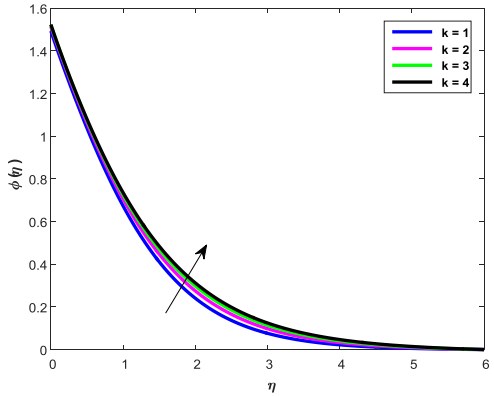

Fig. 18: Nano particle volume fraction profile for different values of k

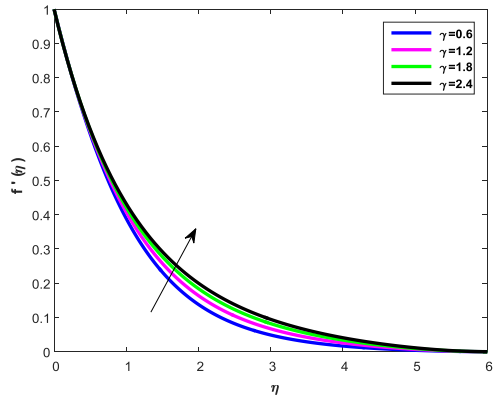

Fig. 19: Velocity profile for different values of γ

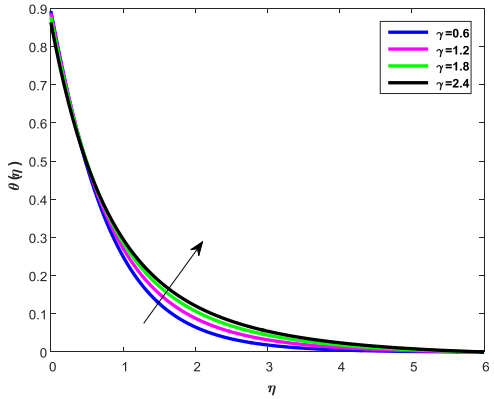

Fig.20:Temperature profile for various values of γ

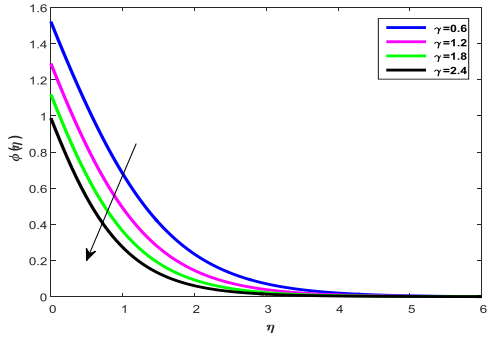

Fig. 21: Nanoparticle volume fraction profile for different values of γ

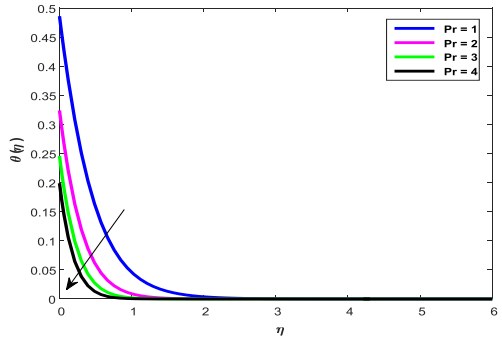

Fig.22:Temperature profile for various values of Pr

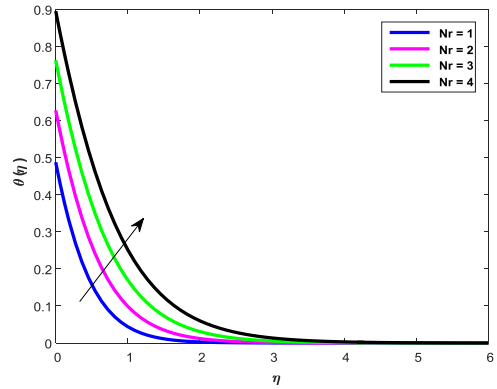

Fig.23:Temperature profile for various values of Nr

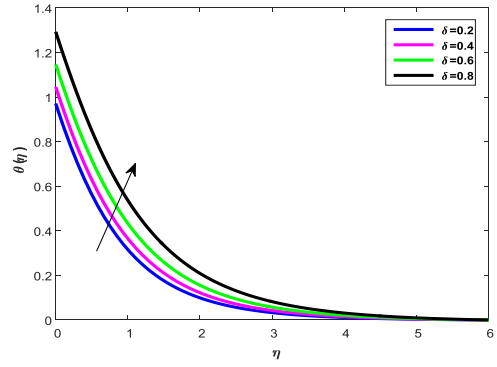

Fig.24:Temperature profile for different values of δ

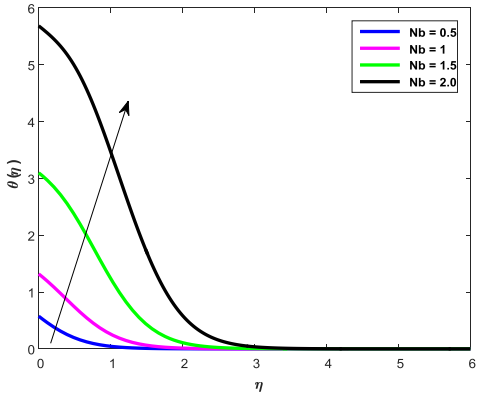

Fig.25:Temperature profile for various values of Nb

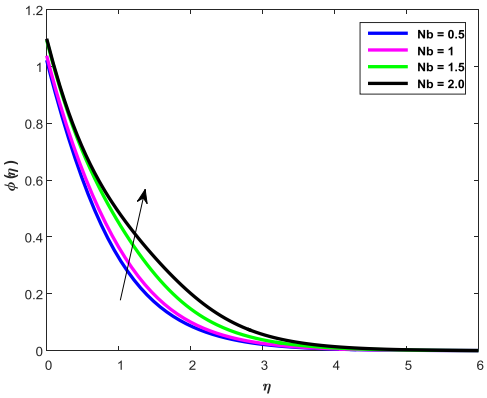

Fig. 26: Nanoparticle volume fraction profile for different values of Nb

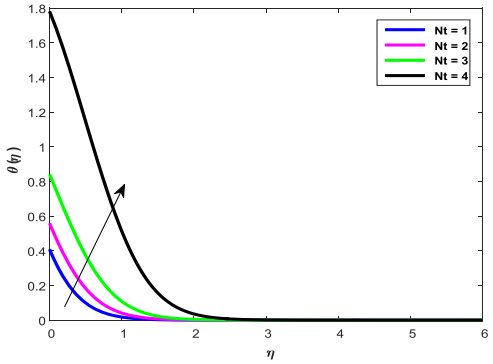

Fig.27:Temperature profile for various values of Nt

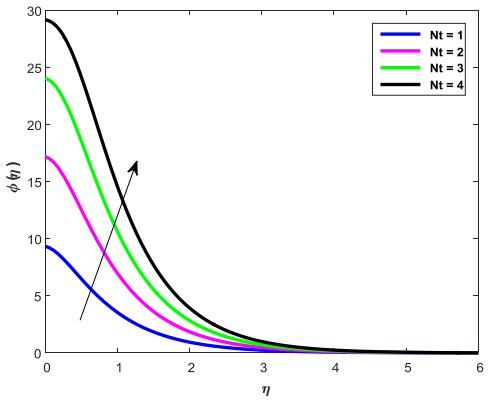

Fig. 28: Nano particle volume fraction profile for different values of Nt

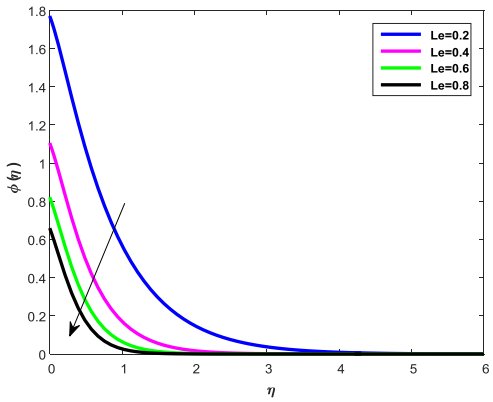

Fig. 29: Nano particle volume fraction profile for different values of Le

VI. CONCLUDING REMARKS

An investigation is performed to peruse the prescribed heat and mass flux conditions on MHD laminar flow of third grade fluid subject to thermal radiation and heat source/sink with nanoparticles. Influence of nanoparticle characteristics viz, thermophoresis and Browning motion are perused. The salient features of present probe are summarized as below

- Variation of M and k on the temperature distribution and nanoparticle concentration are similar.
- The variation of $\alpha_1^*, \alpha_2^*, \beta$ *and* Re on velocity is field is quite paradoxical to temperature and nanoparticle volume fraction.
- Impact of Nt and Nb on temperature distribution are same.
- The larger values of thermal radiation parameter depict greater temperature and thickness of thermal boundary layer.

REFERENCES

[1]. RS Rivlin, JLV Ericksen, Stress-deformation relations for isotropic materials, Journal of Rational Mechanics and Analysis, Vol. 4, pp. 323-425, (1955).
[2]. T. Hayat, R. Zaz, A. Alsaedi and M.M. Rashidi, Hydromagnetic rotating flow of third grade fluid, Applied Mathematics and Mechanics, Vol. 34(12), pp. 1481-1494, (2013).
[3]. M. Zeb, S. Islam, A.M. Siddiqui and T. Haroon, Analysis of third-grade fluid in helical screw rheometer, Journal of Applied Mathematics, Vol. 2013, Article ID 620238, 11 pages, (2013).
[4]. S.N. Majhi and V.R. Nair, Flow of third grade fluid through stenosed tubes, Proceeding of Indian National Science Academy, Vol. 60 (3), pp. 535-542, (1994).
[5]. Taza Gul, Saed Islam, Rehan Sli Shah, Ilyas Khan and Sharidan Shafie, Thin Film Flow in MHD Third Grade Fluid on a Vertical Belt with Temperature Dependent Viscosity, PLOS ONE, Vol. 9(6), e97552, (2014).
[6]. A. Rehman, S. Nadeem and M.Y. Malik, Boundary layer stagnation-point flow of a third grade fluid over an exponentially stretching sheet, Brazilian Journal of Chemical Engineering, Vol. 30(3), pp. 611-618, (2013).
[7]. V. Nagendramma, R.V.M.S.S. Kiran Kumar, P. Durga Prasad, A. Leela Ratnam and S. Vijaya Kumar Varma, Themodiffusion effects on MHD boundary layer slip flow of nanofluid over a nonlinear stretching sheet through a porous medium, Journal of Porous Media, Vol. 20(11), pp. 961-970, (2017).
[8]. Manoj Kumar Nayak, Gauranga Charan Dash and Lambodar Prased Singh, Heat and mass transfer effects on MHD viscoelastic fluid over a stretching sheet through porous medium in presence of chemical reaction, Propulsion and Power Research, Vol. 5(1), pp. 70-80, (2016).
[9]. Muhammad Zubair Akbar, Muhammad Ashraf, Muhammad Farooq Iqbal, *and* Kashif Ali, Heat and mass transfer analysis of unsteady MHD nanofluid flow through a channel with moving porous walls and medium, AIP Advances **6**, 045222 (2016)
[10]. Ali Montakhab, Convective Heat Transfer in Porous Media, Journal of Heat transfer, Vol. 101(3), pp. 501-510, (2010).
[11]. Alibakhsh Kasaeian, Reza Daneshazarian, Omid Mahian, Lioua Kolsi, Ali J. Chamkha, Somchai Wongwises and Ioan Pop, Nanofluid flow and heat transfer in porous media: A review of the latest developments, International Journal of Heat and Mass Transfer, Vol. 107, pp. 778-791 (2017).
[12]. F. M. Abbasi, S. A. Shehzad, T. Hayat, A. Alsaedi, *and* Mustafa A. Obid, Influence of heat and mass flux conditions in hydromagnetic flow of Jeffrey nanofluid, AIP Advances **5**, 037111 (2015)
[13]. Tasawar Hayat, Arsalan Aziz, Taseer Muhammad and Ahmed Alsaedi, Three-dimensional flow of nanofluid with heat and mass flux boundary conditions, Chinese Journal of Physics, Vol. 55 (4), pp. 1495-1510, (2017).
[14]. A. Majeed, T. Javeed, A. Ghaffari and M.M. Rashidi, Analysis of heat transfer due to stretching cylinder with partial slip and prescribed heat flud: A Chebyshev Spectral Newton Iterative Scheme, Alexandria Engineering Journal, Vol. 54, pp. 1029-1036, (2015).
[15]. R. L. Fosdick and K. R. Rajagopal, Anomalous features in the model of second order fluids. Archive for Rational Mechanics and Analysis, Vol. 70**,** pp. 145–152, (1979).
[16]. A. V. Kuznetsov, D. A. Nield, The cheng-minkowycz problem for natural convective boundary layer flow in a porous medium saturated by a nanofluid: A revised model, International Journal of Heat and Mass Transfer, Vol. 65, pp. 682–685, (2013).